

See discussions, stats, and author profiles for this publication at: <https://www.researchgate.net/publication/236913748>

Fundamental Studies of Methyl Iodide Adsorption in DABCO Impregnated Activated Carbons

ARTICLE *in* LANGMUIR · MAY 2013

Impact Factor: 4.46 · DOI: 10.1021/la401334d · Source: PubMed

READS

18

4 AUTHORS, INCLUDING:



Erich A Müller

Imperial College London

128 PUBLICATIONS 2,624 CITATIONS

[SEE PROFILE](#)

Fundamental Studies of Methyl Iodide Adsorption in DABCO Impregnated Activated Carbons

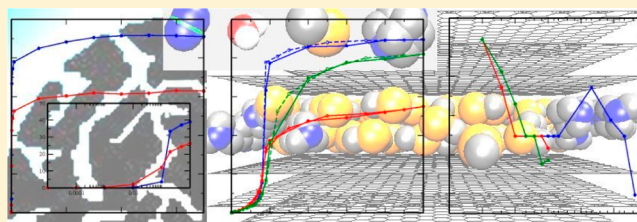
Carmelo Herdes,*[†] Claudia Prosenjak,[‡] Silvia Román,[§] and Erich A. Müller[†]

[†]Department of Chemical Engineering, Imperial College London, South Kensington Campus, London SW7 2AZ, United Kingdom

[‡]Evonik Industries AG, Rodenbacher Chaussee 4, D-63457 Hanau, Germany

[§]Departamento de Física Aplicada, Universidad de Extremadura, Avda. Elvas s/n 06071, Spain

ABSTRACT: Methyl iodide capture from a water vapor stream using 1,4-diazabicyclo[2.2.2]octane (DABCO)-impregnated activated carbons is, for the first time, fundamentally described here on the atomic level by means of both molecular dynamics and grand canonical Monte Carlo simulations. A molecular dynamics annealing strategy was adopted to mimic the DABCO experimental impregnation procedure in a selected slitlike carbon pore. Predictions, restricted to the micropore region, are made about the adsorption isotherms of methyl iodide, water, and nitrogen on both impregnated and bare activated carbon models. Experimental and simulated nitrogen adsorption isotherms are compared for the validation of the impregnation strategy. Selectivity analyses of the preferential adsorption toward methyl iodide over water are also reported. These simulated adsorption isotherms sum up to previous experimental studies to provide an enhanced picture for this adsorption system of widespread use at nuclear plant HVAC facilities for the capture of radioactive iodine compounds.



1. INTRODUCTION

Recently, the removal efficiency of methyl iodide (CH_3I , MeI) by 1,4-diazabicyclo[2.2.2]octane ($\text{C}_6\text{H}_{12}\text{N}_2$, DABCO)-impregnated activated carbon (AC) was experimentally evaluated¹ during the search for alternative carbon precursors in the context of radioactive iodine compound entrapment at nuclear plant HVAC (heating, ventilating, and air conditioning) systems. In that work, different AC samples were characterized by nitrogen, water, and carbon dioxide single adsorption isotherms, mercury porosimetry, and FT-IR spectra.¹ There, the carbon precursor (almond tree pruning, olive stone, both almond and walnut shells), the conditions of physical activation (steam or carbon dioxide under different temperature and activation time conditions), and the DABCO load (specifically at 5% and 10 weight gain) were all separately taken into account. The MeI retention results were explained along the lines of previous findings^{2–5} by hypothesizing that the MeI removal mechanism proceeds via nonspecific (MeI–AC) as well as through specific (MeI–DABCO) interactions without access to MeI adsorption isotherms (which are fundamental to any gas storage and separation process). It is worth noticing that the experimental setup for this specific system is challenging, as one must comply with ASTM D3803-91 (2004) Standard Test Method for Nuclear-Grade Activated Carbon. Also, the disposal of radiolabeled $^{131}\text{ICH}^3$ as well as the subsequent exhausted ACs has to be disposed of in properly sealed nuclear facilities. It is in this context that computer simulations play a leading role in providing pseudoexperimental data and reliable extrapolations of existing data.⁶

The present work, to the best of our knowledge, is the first fundamental molecular-level qualitative prediction of the MeI adsorption behavior in bare and DABCO-impregnated AC (DABCO-AC) models in the presence or absence of water.

We presume a hypothesis commonly employed in tracer studies, namely, that the radioactive nature of the isotope does not change its chemical or physical properties, hence available molecular models and common methodologies for the nonradioactive isotopes can be directly implemented without further specific modifications. We also assume that the general features of a complex carbon matrix may be described as being the integrated result of a local behavior. We use a slit pore of parallel walls as a model for this local environment. A slit pore model is able to predict macroscopic properties quantitatively, such as the different adsorption isotherms at a selected pore size while providing a detailed molecular picture unattainable by experiments.

This work focuses on the prediction of MeI adsorption in DABCO-ACs, capitalizing on previous experimental findings to bring about a more complete understanding of the system.

2. METHODOLOGY

2.1. Molecular Models. Slitlike atomistically detailed carbon pore models were employed. The pore width is fixed at 0.75 nm, the distance defined between the centers of atoms on opposing walls. This value is chosen because it represents the

Received: September 14, 2012

Revised: May 9, 2013

Published: May 16, 2013

mean pore size of common AC, before DABCO impregnation, used in nuclear plant facilities for MeI removal.¹ (See Figure 1

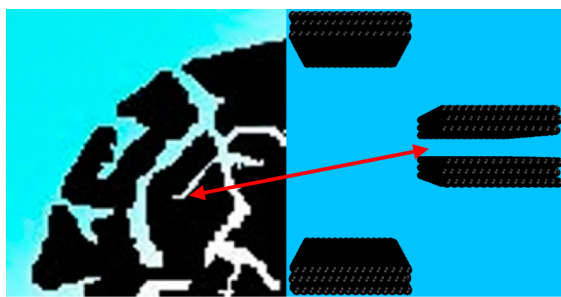


Figure 1. Schematic representation of an AC particle and the simulation cell used.

for schematic representation of an AC particle and a proposed slit-like pore.) The pore walls were described by an array of carbon-atom layers, with periodic boundary conditions in the x and y directions. Each wall is composed of three graphite layers with an interlayer spacing of 0.335 nm.⁷

The adsorbates involved in this study are nitrogen, water, and MeI. Nitrogen molecules were modeled by a pairwise additive potential composed of two negatively charged Lennard-Jones (LJ) sites in which neutrality and an appropriate quadrupole moment are attained by a central massless charged point.⁸ Water molecules are TIP4P type,⁹ a four-site model with one LJ oxygen, two LJ hydrogens, and one massless point of negative charge that is moved off center from the oxygen by 0.015 nm toward the interior bisector of angle HOH. The MeI dumbbell molecule consists of a methyl pseudoatom and an iodine atom separated by the experimental bond length of 0.216 nm. The interaction between MeI molecules is described as well by a LJ potential plus explicit charges.¹⁰ For DABCO, a united atom model is assembled using the parameters from the TraPPE-UA force field.¹¹ The models are depicted in Figure 2 using the van der Waals radii. The Lorentz–Berthelot mixing rules were applied to calculate the interaction of heteroatomic pairs.

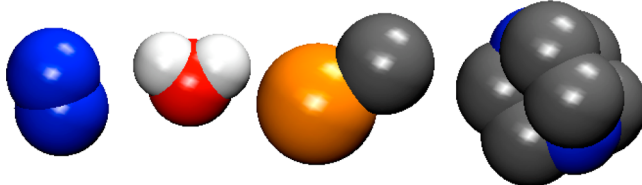


Figure 2. Molecular models used in this work from left to right: nitrogen, water, MeI, and DABCO.

2.2. DABCO-Impregnated Slitlike Carbon Pore by Annealing Molecular Dynamics. The target experimental DABCO-AC is made by sublimating reagent-purity DABCO in a vapor-generating vessel heated to 120 °C.^{1,12} The vapor was diverted from an airtight stainless steel reactor to a reweighed AC bed. After the AC sample cooled, the weight gained was then associated with impregnated DABCO (from 5 to 10%).¹

When GROMACS is used,¹³ a molecular dynamics (MD) annealing temperature scheme is implemented to mimic the experimental impregnation process. In an NVT simulation cell (size $x, y, z = 5.045, 3.815, 2.890$ nm) with periodic boundary conditions and a cutoff of 0.9 nm containing a rigid slitlike carbon pore, we randomly inserted DABCO molecules, up to 1

or 5 wt % DABCO/wt % C, and let the system evolve at 393 K for 5000 ps (time step 2 fs). At this point, the temperature was decreased to 298 K in 1000 ps. After a temperature of 298 K was reached, the system was run for another 5000 ps. (See the temperature and total energy evolution chart on Figure 3 for the 5 wt %/wt % system.) The selected thermostat points were handled by the V-rescale method,¹⁴ the bond and angles were constrained by the Shake method,¹⁵ and the 3D particle mesh Ewald method^{16,17} with 0.12 Fourier spacing was used for the long-range electrostatics calculation.

2.3. Modeling Adsorption Isotherms by Grand Canonical Monte Carlo Simulation. Grand canonical Monte Carlo (GCMC) simulations were carried out using the multipurpose simulation code MuSiC.¹⁸ In the simulations, the carbon pores (and DABCO if present) were considered to be rigid structures (i.e., no further movement of the DABCO molecules was allowed). The sampling protocol included four types of moves—bias insertion and deletion,¹⁸ random rotation and translation—with an equal distribution of weights among the moves. For nitrogen and MeI, 1×10^7 GCMC steps were performed for each point in the adsorption isotherm consecutively (with each step being an attempt to insert, delete, rotate, or translate a molecule) in which half of the steps are taken to equilibrate the system and the other half are taken to sample the data. Water adsorption isotherms needed 2×10^7 GCMC steps for each consecutive simulated point. Given the qualitative character of the present contribution in a single but representative carbon pore size, the adsorption data for water and MeI is presented as absolute fluid density in the pore (number of molecules adsorbed per unit cell) versus fugacity of the bulk phase (in kPa). Meanwhile and for the purpose of validation of the bare and impregnated slitlike carbon pore models, the comparison of simulated and experimental nitrogen adsorption is presented in excess fluid density (STP cm³/g) versus the relative pressure.

We stress that this model is restricted to the micropore region of the activated carbon providing a qualitative description. For a quantitative description of the system a pore size distribution (PSD) approach could be employed in which the adsorption integral equation (AIE) is directly used with a experimental PSD and an appropriate impregnated dense kernel of independent adsorption isotherms to calculate the total experimental isotherm.^{19–21} Alternatively one can use the kernel and the experimental adsorption isotherm to solve (to deconvolute) the AIE for a PSD prediction, if any, of one of the infinite solutions that must be analyzed by physical and mathematical criteria.²² Another approach to a quantitative description could involve the reconstruction of a specific carbon pore structure by a fingerprint model obtained by reverse Monte Carlo²³ or employing disordered realistic representations.²⁴

3. RESULTS AND DISCUSSION

GCMC results and experimental measurements for the nitrogen adsorption isotherms at 77 K in bare AC and DABCO-AC are presented in Figure 4.

All isotherms are type I (IUPAC classification) describing a common micropore filling behavior, as corresponds to the adsorbents typically used in MeI adsorption processes.^{1,25} As expected,^{1,5,26} the DABCO-AC has a lower total adsorption capacity than the bare AC, intrinsically because of the reduction of the available void volume. From the analysis of the experimental adsorption isotherms itself, one can see that the

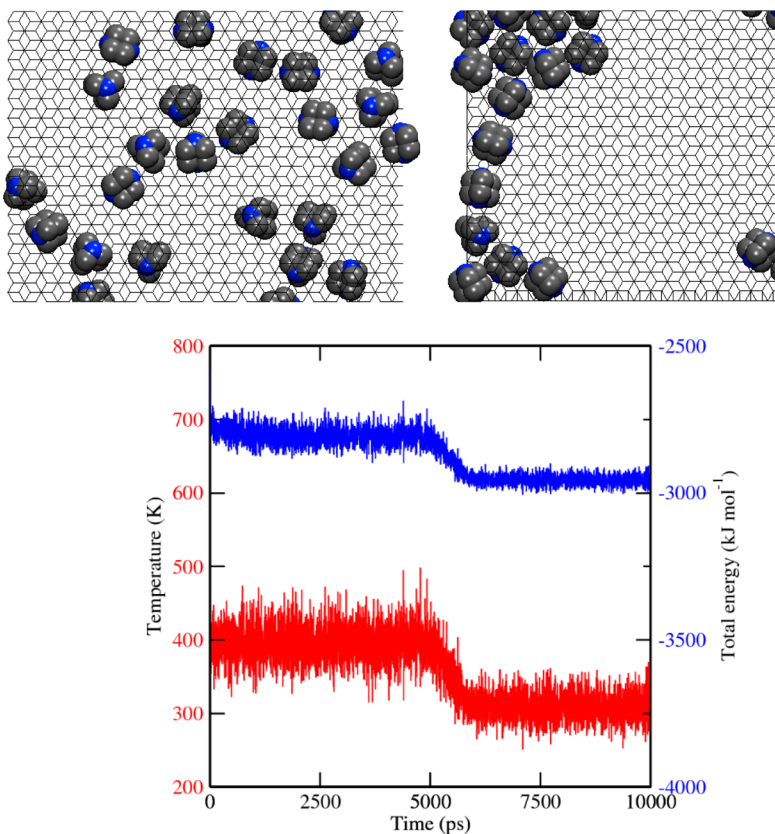


Figure 3. MD snapshots for the initial (left) and the final (right) configurations for 5% DABCO impregnation. The evolution chart for temperature (red curve left-hand y axis) and energy (blue curve right-hand y axis) of the NVT simulation is shown at the bottom.

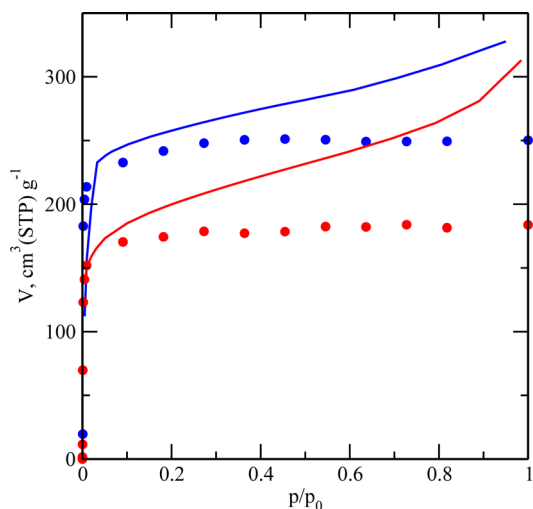


Figure 4. Experimental and simulated nitrogen adsorption isotherms at 77 K in bare AC (blue) and 5% DABCO-AC (red). Solid lines are the experimental measurements, and symbols are the simulated points.

adsorption capacity is higher in the nonimpregnated AC when compared to that in the impregnated one; that is to say, DABCO deposition leads to a specific surface reduction.¹ Despite the fact that the nitrogen volume adsorbed in the nonimpregnated AC decreases with respect to the impregnated one, the shape of the impregnated experimental isotherm remains invariant, reflecting that the impregnation of DABCO took place mainly in the micropore region of the real samples, in accordance with previous results.^{1,25} This is also

quantitatively evident in the reduction of the micropore volume from 0.41 to 0.32 cm³/g; meanwhile, the mesopore volume varies from 0.10 to 0.14 cm³/g in the bare and impregnated carbons, respectively. (See Table 4 in ref 1 for samples S/30 and S/30/S, respectively.) An analogous analysis can be drawn from the simulated adsorption isotherms, reflecting the main adsorption characteristics and trends in their experimental counterparts and restricted to the lower total adsorption capacity of their smaller pore volumes.

Water adsorption isotherms at 298 K presented on/off behavior typical of type V isotherms (see Figure 5).

Below 30 kPa, none of the water molecule can be found in the bare carbon pore; however, at ~35 kPa abrupt condensation takes place and the pore is almost full of water. The 5% DABCO-AC presents an analogous isotherm with delayed pore filling at ~45 kPa. The bottom snapshot (45 kPa) depicts the water in the confined system. This is the expected behavior for a graphite pore with little or no energetic surface heterogeneities²⁷ and suggests that the impregnated DABCO molecules do not act as nucleation sites for the adsorption of water, in spite of the availability of free electron pairs from the nitrogen atoms.

The predicted MeI adsorption isotherms at 298 K in bare AC and 5% DABCO-AC are presented in Figure 6.

They show a type V form with negligible hysteresis. Because a strong interaction does exist between the MeI and DABCO molecules, as a result of chemisorption (mono and dimethyl DABCO quaternary ammonium salt formation²⁸), well-defined hysteresis loops would be expected in the simulated adsorption isotherms, which were not found here. Other contributing factors for hysteresis loops could presumably come from

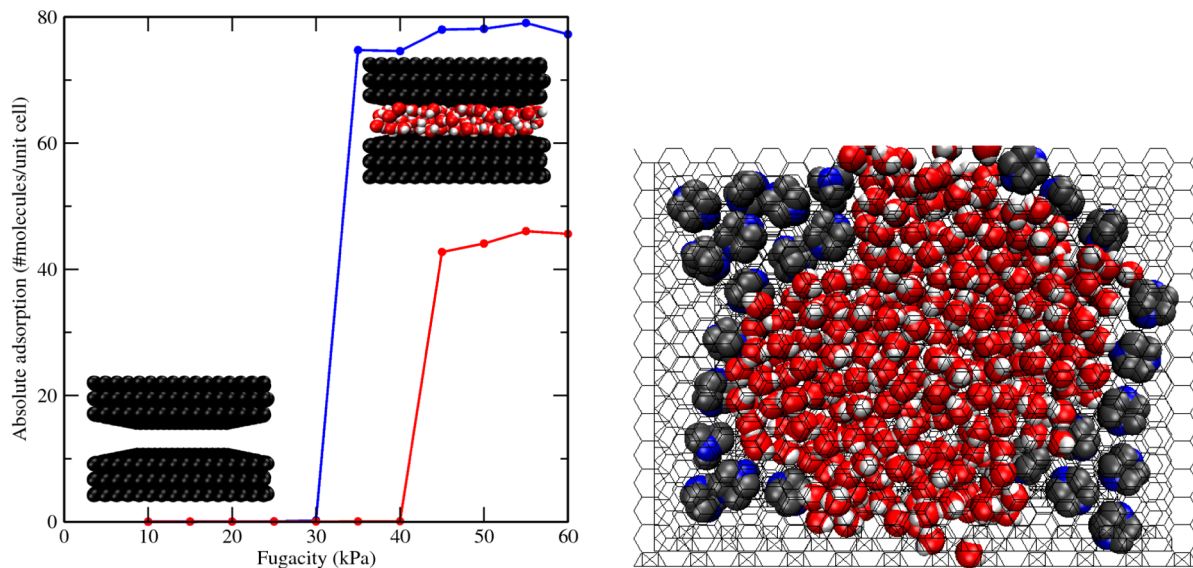


Figure 5. (Left) Predicted water adsorption isotherms at 298 K in bare AC (blue) and 5% DABCO-AC (red). Insets presents snapshots for empty and full bare AC, and solid lines are a guide to the eye. (Right) Snapshot represents the arrangement of water molecules in the DABCO-AC pore after saturation.

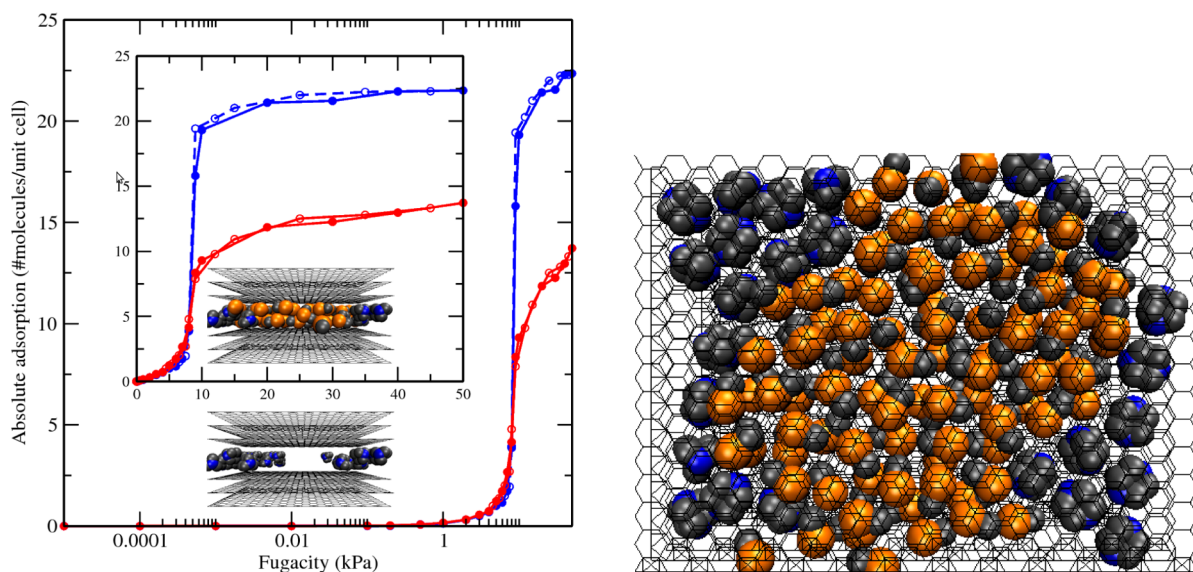


Figure 6. (Left) Predicted MeI adsorption isotherms at 298 K in bare AC (blue) and 5% DABCO-AC (red). Insets present snapshots for empty and saturated AC, and solid lines are a guide to the eye. (Right) Snapshot represent the arrangement of MeI molecules in the DABCO-AC pore after saturation.

entrance effects and kinetics. Additionally, it has been discussed that the differences found between bare AC and DABCO-AC presumably reflect only steric impediments, as a consequence of DABCO molecules blocking the access to the micropores.²⁹ These points are beyond the scope of the current model and point to the limitations of the current model.

At low pressures, the isotherms are convex to the fugacity (pressure) axis, leveling off around 10 kPa. As for the previous adsorptive, the total adsorption capacity for DABCO-AC is less than for bare AC. The adsorption in the low-pressure regime is modestly higher for DABCO-AC. The bottom snapshot depicts the molecular arrangement inside the pore at 45 kPa. It is worth stressing that at this moment the model does not explicitly describe the underlying chemical reaction—mono and dimethyl DABCO quaternary ammonium salt formation,²⁸

however, in the real system the chemisorption contribution has a combined positive effect on the MeI capture.

This far, we have found two different features in the 5% DABCO-impregnated AC models that, if working synergistically, could explain and boost the MeI removal from vapor streams: (i) the delayed water pore filling at ~45 kPa and (ii) the modest higher MeI adsorption at low pressure.

To explore these effects further, we performed a selectivity study in a fully predictive manner for MeI in water with a fixed bulk water molar composition of 0.99 in bare and 5% DABCO-AC. Here we use the common definition of selectivity as the ratio between the molar composition in the pore and the corresponding bulk ratio, $S_{\text{MeI}} = (x_{\text{MeI}}/x_{\text{water}})_{\text{pore}}/(x_{\text{MeI}}/x_{\text{water}})_{\text{bulk}}$. Figure 7 presents these results as a function of the

total fugacity of the system. The gas phase is taken as an ideal gas mixture.

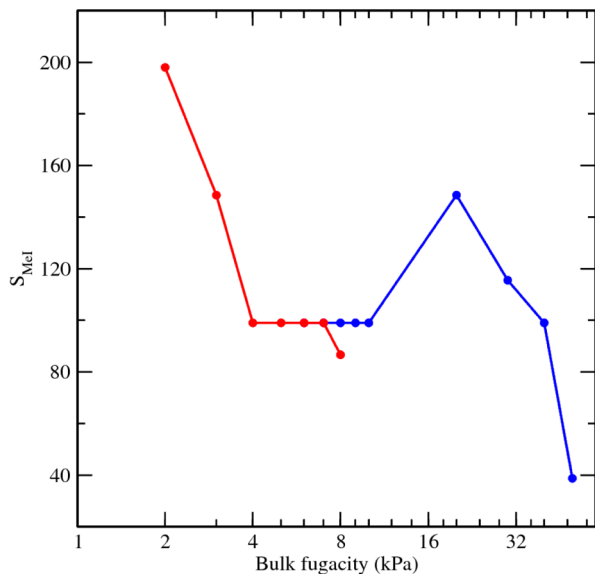


Figure 7. Predicted selectivity for MeI at 298 K in bare AC (blue) and 5% DABCO-AC (red) for a fixed bulk molar composition of 0.99 in water as function of the total bulk fugacity. Solid lines are a guide to the eye.

At 2 kPa, the DABCO-AC sample presents the highest selectivity of ~ 200 , which decreases to ~ 100 at 4 kPa merging with the bare AC selectivity. For fugacities below 2 kPa, it is difficult to ensure good statistics from the GCMC results without considerably increasing the size of the simulation cell. However, such low pressures are not used in HVAC systems. Interestingly, the bare AC itself presents a selectivity of ~ 150 when the total fugacity of the mixture is 20 kPa, decreasing but still being moderately selective to MeI (~ 40) at 50 kPa. This backs our claim that both the delayed water pore filling and the

modest higher MeI adsorption of DABCO-AC work synergistically to increase the selectivity of the system toward MeI capture from vapor streams. Previous findings relate the selectivity of DABCO-AC toward MeI to a decrease in the reversibility of sorption.³⁰

Finally, we present the adsorption and selectivity results obtained when impregnating our model carbon pore with 1% DABCO (Figure 8).

These results point out that the dispersion of DABCO also has a relevant influence on the overall performance of the studied adsorbent, attributed to the better orientation and exposure of the nitrogen atoms in the DABCO molecules, as is evident from the simulations (snapshots in Figure 3) that DABCO is not evenly spread on the pore surface after the impregnation procedure. Presumably, the strong fluid–fluid interactions contribute to local clustering that will have a profound effect on the adsorption behavior of other substances, particular MeI and water. At 1% DABCO-AC, the total adsorption capacity increased and in the low-pressure regime, an enhancement of the selectivity is found (Figure 8). These results give evidence of the importance of optimizing the DABCO impregnation ratio (wt %/wt %) in order to provide the conditions that enhance the selectivity toward CH_3I and also avoid an intrinsic decrease in the pore volume availability resulting from the impregnation procedure. Further work will be devoted to investigating these effects.

4. CONCLUSIONS AND FUTURE WORK

We combined experimental data and molecular simulation results to study the methyl iodide removal mechanism from water vapor in DABCO-impregnated activated carbons at different impregnation levels. Our simulations were carried out in three model pores (nonimpregnated and 1 and 5% DABCO-AC), allowing the first quantitative prediction of the MeI adsorption isotherm and selectivity in the presence of water. We provided additional insights into this system regarding the role of each species on the molecular level. The same procedure will be applied to construct a family of DABCO-AC adsorption

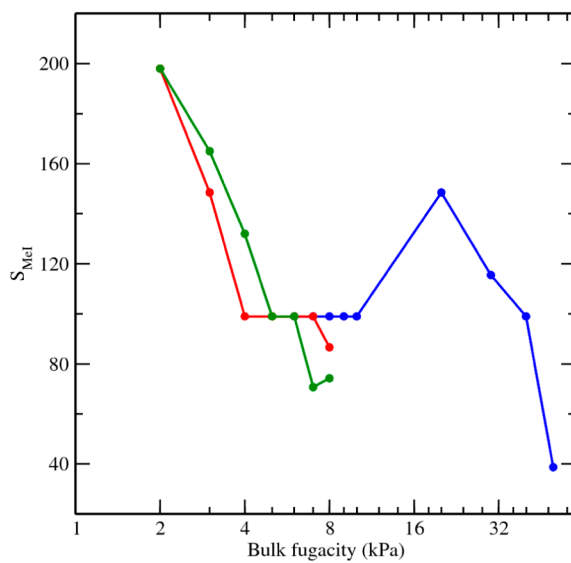
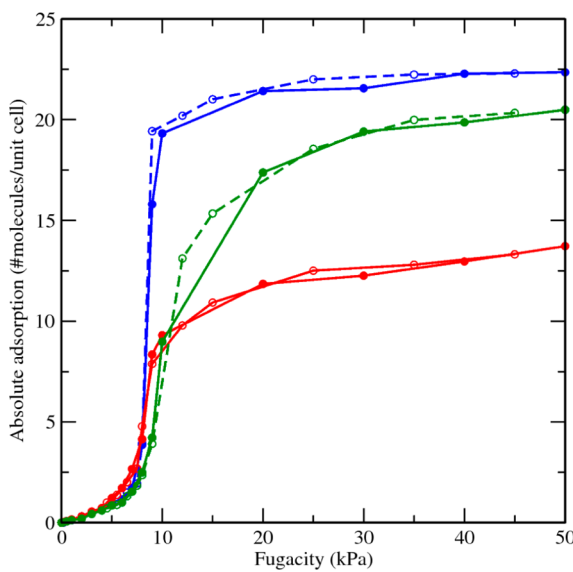


Figure 8. (Left) Predicted MeI adsorption isotherms at 298 K in bare AC (blue), 1% DABCO-AC (green), and 5% DABCO-AC (red). (Right) Selectivity for MeI at 298 K in bare AC (blue), 1% DABCO-AC (green), and 5% DABCO-AC (red) for a fixed bulk molar composition of 0.99 in water as a function of the total bulk fugacity. Solid lines are a guide to the eye.

isotherm curves (a kernel) for the full adsorptive modeling of this system in which the hydrophobic character, the working pressure, and the dispersion of DABCO will be further optimized.

This general methodology could also be used for the study of other relevant impregnants and/or substrates as is the case of silver doped on charcoals, alumina, zeolite, resins, and silica gels, devoted to the removal of radioactive iodide compounds.^{33–34} A silver salt (such as ClAg or NO₃Ag) traps the iodine ions^{32–34} or the organic methyl iodide³³ in a similar fashion as does DABCO (i.e., through a strong chemical interaction, via an ion-exchange reaction), also providing good adsorption selectivity.

AUTHOR INFORMATION

Corresponding Author

*E-mail: c.herdes@imperial.ac.uk.

Notes

The authors declare no competing financial interest.

ACKNOWLEDGMENTS

C.H. and E.A.M. acknowledge financial support from EPSRC (U.K.) through grant EP/I018212 and EP/J014958. We thank João M. V. Nabais (Universidade de Évora, Portugal) for helpful comments and discussions.

REFERENCES

- González-García, C. M.; González, J. F.; Román, S. Removal Efficiency of Radioactive Methyl Iodide on TEDA-Impregnated Activated Carbons. *Fuel Process. Technol.* **2011**, *92*, 247.
- Park, S. W.; Lee, W. K.; Moon, H. Adsorption and Desorption of Gaseous Methyl Iodide in a TEDA Impregnated Carbon Bed. *Sep. Technol.* **1993**, *3*, 133.
- Park, G.; Kim, I.; Lee, J. K.; Ryu, S. K.; Kim, J. H. Effect of the Temperature on the Adsorption and Desorption Characteristics of Methyl Iodide over TEDA-Impregnated Activated Carbon. *Carbon Sci.* **2001**, *2*, 9.
- Laine, J.; Yunes, S. Effect of the Preparation Method on the Pore Size Distribution of Activated Carbon from Coconut Shell. *Carbon* **1992**, *30*, 601.
- Deitz, V. R. Interaction of Radioactive Iodine Gaseous Species with Nuclear Grade Activated Carbons. *Carbon* **1987**, *25*, 31.
- Gubbins, K. E.; Moore, J. D. Molecular Modeling of Matter: Impact and Prospects in Engineering. *Ind. Eng. Chem. Res.* **2010**, *49* (7), 3026.
- Steele, W. A. Physical Interaction of Gases with Crystalline Solids 0.1. Gas-Solid Energies and Properties of Isolated Adsorbed Atoms. *Surf. Sci.* **1973**, *36*, 317.
- Herdes, C.; Lin, Z.; Valente, A.; Coutinho, J. A. P.; Vega, L. F. Nitrogen and Water Adsorption in Aluminum Methylphosphonate Alpha: A Molecular Simulation Study. *Langmuir* **2006**, *22*, 3097.
- Jorgensen, W. L.; Chandrasekhar, J.; Madura, J. D.; Impey, R. W.; Klein, M. L. Comparison of Simple Potential Functions for Simulating Liquid Water. *J. Chem. Phys.* **1983**, *79*, 926.
- Martins-Freitas, F. F.; Silva-Fernandes, F. M. S.; Costa-Cabral, B. J. Vapor-Liquid Equilibrium and Structure of Methyl Iodide Liquid. *J. Phys. Chem.* **1995**, *99*, 5180.
- Wick, C. D.; Stubbs, J. M.; Rai, N.; Siepmann, J. I. Transferable Potentials for Phase Equilibria. 7. Primary, Secondary, and Tertiary Amines, Nitroalkanes and Nitrobenzene, Nitriles, Amides, Pyridine, and Pyrimidine. *J. Phys. Chem. B* **2005**, *109*, 18974.
- González, J. F.; Román, S.; González, C. M.; Ramiro, A. Carbonos Activados y su Procedimiento de Obtención. Patente de Invención no. 2347125.
- Hess, B.; Kutzner, C.; van der Spoel, D.; Lindahl, E. GROMACS 4: Algorithms for Highly Efficient, Load-Balanced, and Scalable Molecular Simulation. *J. Chem. Theory Comput.* **2008**, *4*, 435.
- Bussi, G.; Donadio, D.; Parrinello, M. Canonical Sampling through Velocity Rescaling. *J. Chem. Phys.* **2007**, *126*, 014101.
- Ryckaert, J. P.; Cicotti, G.; Berendsen, H. J. C. Numerical-Integration of Cartesian Equations of Motion of a System with Constraints - Molecular-Dynamics of n-Alkanes. *J. Comput. Phys.* **1977**, *23*, 327.
- Darden, T.; York, D.; Pedersen, L. Particle Mesh Ewald - An N.Log(N) Method for Ewald Sums in Large Systems. *J. Chem. Phys.* **1993**, *98*, 10089.
- Essmann, U.; Perera, L.; Berkowitz, M. L.; Darden, T.; Lee, H.; Pedersen, L. G. A Smooth Particle Mesh Ewald Method. *J. Chem. Phys.* **1995**, *103*, 8577.
- Gupta, A.; Chempath, S.; Sanborn, M. J.; Clark, L. A.; Snurr, R. Q. Object-Oriented Programming Paradigms for Molecular Modeling. *Mol. Simul.* **2003**, *29*, 29.
- Prosenjak, C.; Nabais, J. M. V.; Laginhas, C. E.; Carrott, P. J. M.; Ribeiro-Carrott, M. M. L. Simulations of Phenol Adsorption onto Activated Carbon and Carbon Black. *Adsorp. Sci. Technol.* **2010**, *28*, 797.
- da Costa, J. M. C. P.; Cracknell, R. F.; Seaton, N. A.; Sarkisov, L. Towards Predictive Molecular Simulations of Normal and Branched Alkane Adsorption in Carbonaceous Engine Deposits. *Carbon* **2011**, *49*, 445.
- Jorge, M.; Seaton, N. A. Predicting Adsorption of Water/Organic Mixtures using Molecular Simulation. *AIChE J.* **2003**, *49*, 2059.
- Herdes, C.; Santos, M. A.; Medina, F.; Vega, L. F. Pore Size Distribution Analysis of Selected Hexagonal Mesoporous Silicas by Grand Canonical Monte Carlo Simulations. *Langmuir* **2005**, *21*, 8733.
- Jain, S. K.; Pellenq, R. J. M.; Pikunic, J. P.; Gubbins, K. E. Molecular Modeling of Porous Carbons using the Hybrid Reverse Monte Carlo Method. *Langmuir* **2006**, *22*, 9942.
- Kumar, K. V.; Salih, A.; Lu, L. H.; Muller, E. A.; Rodríguez-Reinoso, F. Molecular Simulation of Hydrogen Physisorption and Chemisorption in Nanoporous Carbon Structures. *Adsorp. Sci. Technol.* **2011**, *29*, 799.
- Chinn, M. J.; Norman, P. R.; Barnes, P. A.; Dawson, E. A. The Influence of Deposition Rate on Impregnant Utilisation. *CARBON*, **1999**, American Carbon Society, Proceedings 24th Biennial Conference, Charleston, SC, July 11–16.
- Kopeční, M. M.; Comor, J. J.; Todorovi, M.; Vujišić, L.; Vucković, D. J. Adsorption of Methyl-Iodide and Normal-Hexane on Fibrous Carbon Materials. *J. Colloid Interface Sci.* **1990**, *134*, 376.
- Muller, E. A.; Gubbins, K. E. Molecular Simulation Study of Hydrophilic and Hydrophobic Behavior of Activated Carbon Surfaces. *Carbon* **1998**, *36*, 1433.
- Ross, M. M.; Kidwell, D. A.; Campana, J. E. Analysis of Impregnated Charcoals by Desorption Ionization Mass-Spectrometry. *Anal. Chem.* **1984**, *56*, 2142.
- Ecob, C. M.; Clements, A. J.; Flaherty, P.; Griffiths, J. G.; Nacapricha, D.; Taylor, C. G. Effect of Humidity on the Trapping of Radioiodine by Impregnated Carbons. *Sci. Total Environ.* **1993**, *130*, 419.
- Ampelogova, N. I.; Kritskii, V. G.; Krupennikova, N. I.; Skortsov, A. I. Carbon-Fiber Adsorbent Materials for Removing Radioactive Iodine from Gases. *At. Energy* **2002**, *92*, 336.
- Chapman, K. W.; Chupas, P. J.; Nenoff, T. M. Radioactive Iodine Capture in Silver-Containing Mordenites through Nanoscale Silver Iodide Formation. *J. Am. Chem. Soc.* **2010**, *132*, 8897.
- Karanfil, T.; Moro, E. C.; Serkiz, S. M. Development and Testing of a Silver Chloride-Impregnated Activated Carbon for Aqueous Removal and Sequestration of Iodide. *Environ. Technol.* **2005**, *26*, 1255.
- Hoskins, J. S.; Karanfil, T. Removal and Sequestration of Iodide using Silver-Impregnated Activated Carbon. *Environ. Sci. Technol.* **2002**, *36*, 784.

- (34) Zhang, H.; Gao, X.; Guo, T.; Li, Q.; Liu, H.; Ye, X.; Guo, M.; Wu, Z. Adsorption of Iodide Ions on a Calcium Alginate–Silver Chloride Composite Adsorbent. *Colloids Surf, A* **2011**, *386*, 166.
- (35) Kikuchi, M.; Kitamura, M.; Yusa, H.; Horiuchi, S. Removal of Radioactive Methyl-Iodide by Silver Impregnated Alumina and Zeolite. *Nucl. Eng. Des.* **1978**, *47*, 283.